energies

MDPI

Article

Sliding Mode Control with Minimization of the Regulation Time in the Presence of Control Signal and Velocity Constraints

Mateusz Pietrala, Piotr Leśniewski * and Andrzej Bartoszewicz

Institute of Automatic Control, Łódź University of Technology, 18/22 Bohdana Stefanowskiego St., 90-924 Łódź, Poland; mateusz.pietrala@p.lodz.pl (M.P.); andrzej.bartoszewicz@p.lodz.pl (A.B.)
* Correspondence: piotr.lesniewski@p.lodz.pl; Tel.: +48-426-312-560

Abstract: In this paper, the design of the terminal continuous-time sliding mode controller is presented. The influence of the external disturbances is considered. The robustness for the whole regulation process is obtained by adapting the time-varying sliding line. The representative point converges to the demand state in finite time due to the selected shape of the nonlinear switching curve. Absolute values of control signal, system velocity and both of these quantities are bounded from above and considered as system constraints. In order to evaluate the dynamical performance of the system, the settling time is selected as a quality index and it is minimized. The approach presented in this paper is particularly suited for systems in which one state (or a set of states) is the derivative of the other state (or a set of states). This makes it applicable to a wide range of electromechanical systems, in which the states are the position and velocity of the mechanical parts.

Keywords: sliding mode control; time-varying sliding line; reaching phase elimination; robust control; finite time convergence; settling time minimization

check for updates

Citation: Pietrala, M.; Leśniewski, P.; Bartoszewicz, A. Sliding Mode Control with Minimization of the Regulation Time in a Presence of Control Signal and Velocity Constraints. *Energies* **2021**, *14*, 2887. https://doi.org/10.3390/en14102887

Academic Editor: Mojtaba Ahmadieh Khanesar

Received: 15 April 2021
Accepted: 10 May 2021
Published: 17 May 2021

Publisher's Note: MDPI stays neutral with regard to jurisdictional claims in published maps and institutional affiliations.

Copyright: © 2021 by the authors. Licensee MDPI, Basel, Switzerland. This article is an open access article distributed under the terms and conditions of the Creative Commons Attribution (CC BY) license (https://creativecommons.org/licenses/by/4.0/).

1. Introduction

Sliding mode control has become an efficient regulation control approach due to its robustness to perturbations and computational efficiency [1–6]. First mentions about continuous-time systems can be found in the Russian literature [7]. Then, this strategy was developed in order to apply it to discrete-time systems [8–10]. Sliding mode control can be split into two stages: the reaching and the sliding phase. In the first one, the representative point (state vector) moves in the direction of the so-called sliding hypersurface or its vicinity. In this phase, the system is vulnerable to an influence of the external disturbances. Then, in the sliding phase, the system becomes insensitive to these perturbations. Hence, in order to obtain insensitivity to external disturbances for the entire control process, time-variant sliding hypersurfaces can be introduced [11,12]. One of the reaching phase elimination techniques is to select this hyperplane in such a manner that at the initiation of the control process, it crosses both the initial and the demand state. Furthermore, two strategies can be considered: when the switching hyperplane stops during the control process and when it moves for the whole regulation process. One of the primary goals of sliding mode control is to obtain a satisfying dynamical performance and guarantee a stable sliding motion. In most cases, it is ensured that one of two methods is used: pole placement or optimal control. Furthermore, it is also important to achieve the convergence of the representative point to the demand state in finite time. Hence, the sliding hypersurface has to be nonlinear [13–15]. Otherwise, the convergence would only be asymptotic. Another important issue is to evaluate the dynamical performance of the control loop. It can be obtained by minimizing one of well-known quality indices used in automation, for example: regulation time, integral absolute error (IAE), integral square error (ISE), integral time absolute error (ITAE), integral time-multiplied square error (ITSE). Aiming at practical applications of the proposed strategy constraints must be imposed on signals such as

control signal, position, velocity, etc. [16,17]. Of course, these limitations can be combined in order to achieve desirable properties.

Due to the advantages outlined above, sliding mode control is often used in practice, especially in power converter systems and electric drives. In [18], the super twisting sliding mode control of synchronous machines with permanent magnets is studied. The authors proposed a so-called ultra-local model of the permanent magnet synchronous motor. The proposed model is relatively uncomplicated, which allows the system to work, without the necessity of determining the exact specification of the synchronous motor parameters. A parameter of the model is then adjusted online. The authors, instead of applying a classic state observer, proposed its variation, called the smoothing extended state observer. This allows to minimize the fluctuations in the estimation of the state variable. Computer simulations and experiments on a test setup demonstrate the superiority of the approach, namely the reduced oscillations and quicker response. The work [19] also analyzes the control of electric drive systems with sliding modes, namely controlling the speed of an induction motor. The derived method of control has important advantages when compared to a classical proportional–integral controller. It has less overshoot and better robustness with respect to external perturbations. Controlling an induction motor has also been the topic of [20]. In that work, a six-phase induction motor is controlled in a cascade structure, with a PI speed controller and the proposed terminal sliding mode current controller. It has been shown that by using a nonlinear sliding hyperplane, one can reduce the control time. Results were verified on a real 2 kW motor. On the other hand, in [21], an integral terminal sliding mode controller was proposed for the control of wireless charging systems. The charging circuit on the receiver side stores power not only in the battery, but in a supercapacitor bank as well. Thanks to this, the proposed controller can ensure that the energy transfer is performed with the maximum possible efficiency. The controller performance was verified by computer simulations and hardware in the loop tests. The methodology of time-varying sliding hyperplanes was utilized in [22] to control a DC–DC buck converter, which allowed to obtain robustness for the whole control process. To limit the switching frequency, the authors introduced a hysteresis function into the control signal. This, on one hand, is beneficial, as the switching frequency automatically shifts, to ensure the control precision predetermined by the hysteresis band. On the other hand, it is well known that varying the switching frequency in this manner can have unpleasant auditory effects. When dealing with control systems in which maintaining constraints is one of the main factors, model predictive control (MPC) [23,24] is one of the main solutions. However, it has some drawbacks, as it requires online optimization, which makes it difficult to apply to complex systems with short time constants (as the computational power required to perform the optimization can become prohibitively expensive in these cases). The approach proposed in this paper, on the other hand, requires some initial "off-line" optimization; however, after that, it does not require significant computational effort in the control loop.

This paper is organized as follows. Sections 2 and 3 contain the main results of the paper. At first, the sliding mode controller was designed. Furthermore, the admissible set of the sliding line parameters was derived in three cases: when the absolute value of the control signal is constrained, when the absolute value of system's velocity is constrained and when both of these limitations are simultaneously taken into account. Then, the minimization of the settling time in three scenarios mentioned before was performed. A simulation example presented in Section 4 verifies the theoretical considerations. Section 5 concludes the paper.

2. Sliding Mode Controller Design

In this section, we will present the design of the sliding mode controller for the second order continuous-time system. A nonlinear, time-varying switching hyperplane will be selected in such a manner that the reaching phase will be eliminated. In this way, the robustness to the external disturbances is guaranteed for the whole regulation process.

Moreover, the finite time convergence to the demand state will be achieved. Furthermore, we will derive the admissible set of the sliding line parameters in three cases:

1. When the magnitude of the control signal is constrained;
2. When the magnitude of the system's velocity is constrained;
3. When the magnitude of the control signal and the absolute value of the system's velocity are both constrained.

The dynamical performance of the control loop will be evaluated by minimizing the regulation time, which is a well-known quality index commonly used in control engineering. In this way, the system state will arrive at the set point in the shortest possible time. As for almost all systems, the highest energy efficiency is achieved in the steady set point, which will limit the energy losses in the system. Let us consider a second order dynamical system described by the following state equations:

$$\begin{cases} \frac{d}{dt}\zeta_1(t) = \zeta_2(t) \\ \frac{d}{dt}\zeta_2(t) = f(\zeta_1(t), \zeta_2(t), t) + d(t) + bu(t) \end{cases}, \tag{1}$$

where $\zeta_1(t)$ is the system's position, $\zeta_2(t)$ is the system's velocity and f is an unknown function of time, position and velocity. External disturbances are denoted as d. We require that f and d are bounded, so that the absolute value of their sum fulfills the following condition:

$$|f(\zeta_1(t), \zeta_2(t), t) + d(t)| \leq M, \tag{2}$$

where M is a known a priori. Control signal u is related to a scalar b. Our aim was to design a sliding mode controller that enforces a stable sliding motion along a time-variant switching curve and ensures the convergence from the initial point $\zeta_1(0) \neq 0, \zeta_2(0) = 0$ to the desired point $(0, 0)$ in finite time. In order to remove the reaching phase and obtain the robustness for the entire control process, we choose the following sliding variable:

$$s(t) = c(t)\text{sgn}(\zeta_1(t))\sqrt{|\zeta_1(t)|} + \zeta_2(t), \tag{3}$$

where

$$c(t) = \begin{cases} \iota t & \text{for} \quad t \leq t_0 \\ \iota t_0 & \text{for} \quad t > t_0 \end{cases}. \tag{4}$$

Parameter $\iota > 0$ determines the movement speed of the sliding line given by $s(t) = 0$ and t_0 is the moment in which that line stops and remains fixed until the end of the control process. The values of parameters ι and t_0 will be selected, based on the minimization of the regulation time, for different constraints imposed on the system, in the following subsections of this paper. The sign function is equal to 1 for positive arguments, equal to 0 for 0 and -1 for negative arguments. Substituting $t = 0$ to the Equation (3) we obtain:

$$s(0) = \zeta_2(0) + c(0)\text{sgn}(\zeta_1(0))\sqrt{|\zeta_1(0)|} = 0, \tag{5}$$

so we can conclude that for $t = 0$ the representative point is placed on the switching curve, which results in elimination of the reaching phase and robustness to the external disturbances for the whole regulation process. In order to achieve a stable sliding motion, we select the following control signal

$$u(t) = -\frac{1}{b}\left[\text{sgn}(\zeta_1(t))\sqrt{|\zeta_1(t)|}\frac{d}{dt}c(t) + M\text{sgn}(s(t)) + \frac{\zeta_2(t)c(t)}{2\sqrt{|\zeta_1(t)|}}\right]. \tag{6}$$

Theorem 1. *The control signal (6) ensures a stable sliding motion for the entire regulation process.*

Proof. In order to prove that the stable sliding motion is achieved for the whole regulation process, we have to show that the inequality:

$$s(t)\frac{d}{dt}s(t) \leq 0 \tag{7}$$

is true for any $t > 0$. Let us observe that typically, the inequality in (7) must be strict, to ensure the convergence to the sliding hyperplane. However, in our approach, the initial value of the sliding variable is zero. Therefore, non-strict inequality is sufficient to ensure the sliding motion. Calculating the derivative of the sliding variable (3), we obtain:

$$\frac{d}{dt}s(t) = \frac{d}{dt}\zeta_2(t) + \mathrm{sgn}(\zeta_1(t))\sqrt{|\zeta_1(t)|}\frac{d}{dt}c(t) + \frac{c(t)\zeta_2(t)}{2\sqrt{|\zeta_1(t)|}}. \tag{8}$$

Using the second equation in (1) and the control signal (6), we can rewrite Equation (8) as follows:

$$\frac{d}{dt}s(t) = f(\zeta_1(t), \zeta_2(t), t) + d(t) - M\mathrm{sgn}(s(t)). \tag{9}$$

Let us consider three cases:

1. $s(t) < 0$.
   In this case, Equation (9) is of the form:

$$\frac{d}{dt}s(t) = f(\zeta_1(t), \zeta_2(t), t) + d(t) + M. \tag{10}$$

   Using inequality (2), we obtain that the derivative of the sliding variable is always non-negative. Therefore, inequality (7) is true for any $t > 0$.
2. $s(t) = 0$.
   In this case, the product of the sliding variable and its derivative is always equal to 0. Hence, inequality (7) is fulfilled for any $t > 0$.
3. $s(t) > 0$.
   When the sliding variable is positive, then the Equation (9) can be rewritten as

$$\frac{d}{dt}s(t) = f(\zeta_1(t), \zeta_2(t), t) + d(t) - M. \tag{11}$$

   Again, using inequality (2), we obtain that the derivative of the sliding variable is non-positive. Therefore, the inequality (7) is always true.

In summary, the inequality (7) is fulfilled for any sign of the sliding variable, which ends the proof. □

3. Optimization of the Controller Parameters

In this section, we will derive admissible sets of parameters ι and t_0 related to the switching curve in the presence of three types of constraints enumerated in this section. Moreover, we will consider two possible scenarios:

1. The sliding line moves, then it stops and stays stationary until the control process finishes;
2. The sliding line moves during the entire control process.

At first, we must derive equations for both state variables. Theorem 1 has shown that the proposed control signal ensures stable sliding motion for the whole regulation process, i.e., the representative point remains on the switching curve $s(t) = 0$. From this fact and Equation (3), we obtain that the system's velocity is given as

$$\zeta_2(t) = -c(t)\mathrm{sgn}(\zeta_1(t))\sqrt{|\zeta_1(t)|}. \tag{12}$$

Therefore, our first step is to derive an equation for $\sqrt{|\zeta_1(t)|}$. Substituting the Formula (12) to the first equation in (1), we obtain

$$c(t)\text{sgn}(\zeta_1(t))\sqrt{|\zeta_1(t)|} + \frac{d}{dt}\zeta_1(t) = 0. \tag{13}$$

Using the substitution $y(t) = \sqrt{|\zeta_1(t)|}$, we solve the above differential equation obtaining that in the first case:

$$\sqrt{|\zeta_1(t)|} = \begin{cases} C_1 - \frac{\iota t^2}{4} & \text{for} \quad t \leq t_0 \\ C_2 - \frac{\iota t_0 t}{2} & \text{for} \quad t_0 < t < t_f \\ 0 & \text{for} \quad t \geq t_f \end{cases}. \tag{14}$$

Positive parameters C_1 and C_2 are constants acquired during the integration process and t_f is the regulation time. From the fact that $\sqrt{|\zeta_1(t)|}$ is continuous, we can calculate these parameters. Deriving the limits of the function (14) in points $0, t_0$ and t_f, we obtain:

1. $t = 0$.
   In this case, we obtain:
   $$C_1 = \sqrt{|\zeta_1(0)|}. \tag{15}$$

2. $t = t_0$.
   The left-hand side limit of $\sqrt{|\zeta_1(t)|}$ in t_0 is equal to $\sqrt{|\zeta_1(0)|} - \frac{1}{4}\iota t_0^2$ and the right-hand side limit is $C_2 - \frac{1}{2}\iota t_0^2$. Hence:
   $$C_2 = \sqrt{|\zeta_1(0)|} + \frac{1}{4}\iota t_0^2. \tag{16}$$

3. $t = t_f$.
   By equating one-sided limits at t_f, we obtain:
   $$\sqrt{|\zeta_1(0)|} + \frac{1}{4}\iota t_0^2 - \frac{1}{2}\iota t_0 t_f = 0. \tag{17}$$

   From the above equation, we obtain the formula describing the regulation time, which is our quality index:
   $$t_f = \frac{1}{2}t_0 + \frac{2\sqrt{|\zeta_1(0)|}}{\iota t_0}. \tag{18}$$

In summary, Equation (14) can be rewritten as follows:

$$\sqrt{|\zeta_1(t)|} = \begin{cases} \sqrt{|\zeta_1(0)|} - \frac{\iota t^2}{4} & \text{for} \quad t \in [0, t_0] \\ \sqrt{|\zeta_1(0)|} + \frac{\iota t_0^2}{4} - \frac{\iota t_0 t}{2} & \text{for} \quad t \in \left(t_0, t_f\right] \\ 0 & \text{for} \quad t \in \left(t_f, \infty\right) \end{cases}. \tag{19}$$

In order to calculate the magnitude of the system's velocity, we substitute (19) to Equation (12), obtaining:

$$|\zeta_2(t)| = \begin{cases} \iota t\sqrt{|\zeta_1(0)|} - \frac{\iota^2 t^3}{4} & \text{for } t \in [0, t_0] \\ \iota t_0\sqrt{|\zeta_1(0)|} + \frac{\iota^2 t_0^3}{4} - \frac{\iota^2 t_0^2 t}{2} & \text{for } t \in \left(t_0, t_f\right] \\ 0 & \text{for } t \in \left(t_f, \infty\right) \end{cases}. \tag{20}$$

In the case where the sliding line is non-stationary during the entire regulation process, we transform Equations (14) and (20), obtaining:

$$\sqrt{|\zeta_1(t)|} = \begin{cases} \sqrt{|\zeta_1(0)|} - \frac{\iota t^2}{4} & \text{for} \quad t \in \left[0, t_f\right] \\ 0 & \text{for} \quad t \in \left(t_f, \infty\right) \end{cases}, \tag{21}$$

$$|\zeta_2(t)| = \begin{cases} \iota t\sqrt{|\zeta_1(0)|} - \frac{\iota^2 t^3}{4} & \text{for } t \in \left[0, t_f\right] \\ 0 & \text{for } t \in \left(t_f, \infty\right) \end{cases}. \tag{22}$$

The regulation time is given as

$$t_f = \frac{2\sqrt[4]{|\zeta_1(0)|}}{\sqrt{\iota}}. \tag{23}$$

3.1. Control Signal Constraint

Our aim is to calculate parameters ι and t_0 for which the absolute value of the control signal will be constrained from above by an a priori known positive parameter $u_{\max}$ for the whole regulation process, meaning that:

$$|u(t)| \leq u_{\max} \tag{24}$$

for any $t \geq 0$. Substituting the control signal (6) into the above inequality, we obtain:

$$\left|\operatorname{sgn}(\zeta_1(t))\sqrt{|\zeta_1(t)|}\frac{d}{dt}c(t) + \frac{\zeta_2(t)c(t)}{2\sqrt{|\zeta_1(t)|}} + M\operatorname{sgn}(s(t))\right| \leq |b|u_{\max}. \tag{25}$$

From the additivity and multiplicativity of the absolute value and Equation (12), we obtain that the magnitude of the control signal is constrained from above by $u_{\max}$ if the inequality:

$$\left|\sqrt{|\zeta_1(t)|}\frac{d}{dt}c(t) - \frac{c^2(t)}{2}\right| \leq |b|u_{\max} - M. \tag{26}$$

is true. In order to derive the admissible set, we will consider two cases. In the first one, we will take into account the time from the moment when the sliding line stops to the end of the regulation process. In the second case, we will consider the movement of the representative point along the moving sliding line.

1. $t > t_0$.
   Using Equation (4), one can observe that function c is constant $c(t) = \iota t_0$. This means that its derivative with respect to time is always equal to 0. Hence, we can rewrite formula (26) as follows:
   $$\frac{\iota^2 t_0^2}{2} \leq |b|u_{\max} - M. \tag{27}$$
   After calculations, we obtain the following inequality for t_0:
   $$t_0 \leq \frac{\sqrt{2(|b|u_{\max} - M)}}{\iota}, \tag{28}$$
   for which the magnitude of the input is constrained from above by the parameter $u_{\max}$. However, the t_0 constraint depends on the parameter ι. Therefore, in order to determine the admissible set of parameters ι and t_0, we have to consider the situation when the state is on the moving sliding line.

2. $t \leq t_0$.
Again, using Equation (4), we obtain $c(t) = \iota t$. Calculating the derivative, we obtain $\frac{d}{dt}c(t) = \iota$. In this case, inequality (26) can be rewritten as

$$\left| \iota \sqrt{|\zeta_1(t)|} - \frac{\iota^2 t^2}{2} \right| \leq |b| u_{\max} - M. \tag{29}$$

From inequality (27), we can conclude that $\left| \frac{\iota^2 t^2}{2} \right| \leq |b| u_{\max} - M$ is true for any $t \leq t_0$. Therefore, inequality (29) holds, when:

$$\left| \iota \sqrt{|\zeta_1(t)|} \right| \leq |b| u_{\max} - M. \tag{30}$$

Using Theorem 1 and the fact that the state converges to the demand state on the sliding line, one can deduce that the first state variable is monotonically increasing or monotonically decreasing, depending on the initial point. Hence:

$$\max_{t \geq 0} |\zeta_1(t)| = |\zeta_1(0)|. \tag{31}$$

Therefore, inequality (30) holds, when the inequality:

$$\left| \iota \sqrt{|\zeta_1(0)|} \right| \leq |b| u_{\max} - M \tag{32}$$

is fulfilled. Let us observe that inequality (32) is equivalent to inequality (29) for $t = 0$, which means that condition (32) does not contain any excess. In summary, the magnitude of the control signal is constrained from the above by $u_{\max}$, if:

$$\iota \leq \frac{|b| u_{\max} - M}{\sqrt{|\zeta_1(0)|}} \tag{33}$$

is true.

In the second scenario, when the sliding line moves for the entire control process, we have to ensure that inequality (29) is true on the boundary of the domain. Let us observe that for $t = 0$, the constraint on ι is of the form (33). If $t = t_f$, then by substituting Equation (23) into inequality (29), we obtain that the control signal is limited, when:

$$\iota \leq \frac{|b| u_{\max} - M}{2\sqrt{|\zeta_1(0)|}}. \tag{34}$$

Let us emphasize that the constraint (34) is more restrictive than inequality (33).

3.2. System's Velocity Constraint

In this subsection, we will derive the admissible set of the sliding line parameters, for which the magnitude of the system's velocity will be limited from above by a known, positive parameter $\zeta_{2\max}$ during the whole regulation process, meaning that:

$$|\zeta_2(t)| \leq \zeta_{2\max} \tag{35}$$

for any $t \geq 0$. Again, two strategies will be taken into account: when the sliding curve moves for the whole regulation process and when that curve stops during the regulation process and then it becomes stationary.

1. Convergence along the moving switching curve.
In this case, our goal is to constrain the system's velocity given by Equation (22). If the state converges to the desired point along the moving switching curve, then the admissible set will consist of only one constraint, as in this case $t_0 = t_f$. The first

step will be deriving the moment t_m in which the velocity reaches its extreme value. Now, the derivative of the first equation in (22) will be calculated and equated to zero, obtaining:

$$\iota\sqrt{|\zeta_1(0)|} - \frac{3}{4}\iota^2 t^2 = 0. \tag{36}$$

Solving this equation for t and taking into account that it has to be positive, we obtain:

$$t_m = \frac{2\sqrt{3}\sqrt[4]{|\zeta_1(0)|}}{3\sqrt{\iota}}. \tag{37}$$

Substituting (37) into the first equation in (22), one can obtain that the maximum absolute value of the system's velocity is given by

$$\max_{t>0}|\zeta_2(t)| = \frac{4\sqrt{3\iota}\sqrt[4]{|\zeta_1(0)|^3}}{9}. \tag{38}$$

Therefore, in order to limit the magnitude of the system's velocity by $\zeta_{2\max}$, inequality:

$$\frac{4\sqrt{3\iota}\sqrt[4]{|\zeta_1(0)|^3}}{9} \leq \zeta_{2\max} \tag{39}$$

has to be satisfied. Hence, the admissible set for the case, when the demand state is reached along the moving switching curve, is given as

$$\iota \leq \frac{27x_{2\max}^2}{16\sqrt{|\zeta_1(0)|^3}}. \tag{40}$$

2. Convergence along the fixed switching curve.
In this case, the representative point reaches the demand state at time $t > t_0$. Let us notice that taking into account the time interval $\left[t_0, t_f\right]$ and the shape of the switching curve, one can conclude that the maximum absolute value of the system's velocity is reached at the time t_0. Therefore, we have yet to consider the case when $t \in [0, t_0]$. In this scenario, the maximum absolute value of the system's velocity will be reached at t_0 or t_m given by (37). Now, let us consider two cases:
   - $t_0 > t_m$.
     If the absolute value of the system's velocity reaches its maximum, before the switching curve stops, then the maximum is reached at the moment t_m given by Equation (37). Therefore, in order to fulfill inequality (35) for any $t > 0$, inequality (40) has also to be true.
   - $t_0 \leq t_m$.
     In this case, the maximum of the absolute value of the system's velocity is reached at $t = t_0$. Let us notice that first formulas in (20) and (22) are the same. Hence, following a similar procedure as in the first scenario, we obtain that the absolute value of the system's velocity is attained at the moment:

$$t_0 = \frac{2\sqrt{3}\sqrt[4]{|\zeta_1(0)|}}{3\sqrt{\iota}} \tag{41}$$

     and similarly, as in the previous scenario, the admissible set is given by (40).

To sum up, in order to limit the magnitude of the system's velocity by $\zeta_{2\max}$ for the whole regulation process, the parameter ι has to satisfy inequality (40).

3.3. Control Signal and System's Velocity Constraints

In this subsection, our goal is to derive an admissible set of the switching curve parameters, for which conditions (24) and (35) are fulfilled. Therefore, inequality (28) has to be true and ι has to satisfy both restrictions (33) and (40). Therefore, the constraint of parameter ι in the case when the sliding line stops during the regulation process can be given by

$$\iota \leq \min\left\{\frac{|b|u_{\max}-M}{\sqrt{|\zeta_1(0)|}}; \frac{27x_{2\max}^2}{16\sqrt{|\zeta_1(0)|^3}}\right\}. \tag{42}$$

When the desired point is reached along the moving switching curve, the admissible set is:

$$\iota \leq \min\left\{\frac{|b|u_{\max}-M}{2\sqrt{|\zeta_1(0)|}}; \frac{27x_{2\max}^2}{16\sqrt{|\zeta_1(0)|^3}}\right\}. \tag{43}$$

3.4. Settling Time Minimization

In this subsection, our goal is to minimize the regulation time—a quality index commonly used in control engineering—in the following three cases:

1. When the magnitude of the control signal is constrained;
2. When the magnitude of the system's velocity is constrained;
3. When the magnitude of the control signal and the absolute value of the system's velocity are both constrained.

In each of these three cases, we derive the optimal parameters ι and t_0 from the admissible sets, for which the regulation time is minimized.

3.4.1. Settling Time Minimization with the Control Signal Constraint

Now, we will derive the minimal regulation time, for which inequality (24) is fulfilled for any $t \geq 0$. Moreover, we will decide which strategy is the most beneficial: the one in which the switching curve stops during the control process or the one in which the sliding line moves for the whole control process.

Theorem 2. *If the absolute value of the control signal is bounded from above by $u_{\max}$ for any $t \geq 0$, then the minimum regulation time is*

$$t_f = \frac{3}{2}\sqrt{\frac{2|\zeta_1(0)|}{|b|u_{\max}-M}} \tag{44}$$

and the optimal sliding line parameter values are:

$$\begin{cases} \iota = \frac{|b|u_{\max}-M}{\sqrt{|\zeta_1(0)|}} \\ t_0 = \sqrt{\frac{2|\zeta_1(0)|}{|b|u_{\max}-M}} \end{cases}. \tag{45}$$

The most beneficial strategy is the one in which the switching curve stops during the regulation process.

Proof. We will consider two possible scenarios: when the switching stops during the control process and when the sliding is non-stationary for the whole regulation process.

1. $t_f > t_0$.
   In this case, the regulation time is given by Equation (18). In order to determine its minimum value, we will consider t_f as a function of ι and t_0. At first, let us calculate the partial derivative of t_f with respect to ι:

$$\frac{\partial t_f}{\partial \iota} = -\frac{2\sqrt{|\zeta_1(0)|}}{\iota^2 t_0}. \tag{46}$$

Taking into account the fact that $\sqrt{|\zeta_1(0)|}, \iota$ and t_0 are positive, we conclude that the right hand side of (46) is always negative. Therefore, the regulation time is a decreasing function with respect to ι and its minimum value is obtained on the edge of the admissible set. Let us consider the maximum admissible value of ι which is equal to:

$$\iota = \frac{|b|u_{\max} - M}{\sqrt{|\zeta_1(0)|}}. \tag{47}$$

Substituting (47) into Equation (18) we obtain:

$$t_f = \frac{1}{2}t_0 + \frac{2|\zeta_1(0)|}{t_0(|b|u_{\max} - M)}. \tag{48}$$

In order to calculate the minimum value of the regulation time, we obtain the derivative of the function (48) with respect to t_0 as follows:

$$\frac{\partial t_f}{\partial t_0} = \frac{1}{2} - \frac{2|\zeta_1(0)|}{t_0^2(|b|u_{\max} - M)}. \tag{49}$$

Equating the above formula to zero, taking into account that $t_0 > 0$ and solving this equation, we obtain that the only stationary point is:

$$t_0 = 2\sqrt{\frac{|\zeta_1(0)|}{|b|u_{\max} - M}}. \tag{50}$$

We have to examine whether the above point belongs to the admissible set. Substituting value (47) into the inequality (28), we obtain:

$$t_0 \leq \sqrt{\frac{2|\zeta_1(0)|}{|b|u_{\max} - M}}. \tag{51}$$

Hence, the value (50) does not belong to the admissible set. Therefore, the minimum value of the regulation time is obtained for:

$$\begin{cases} \iota = \frac{|b|u_{\max} - M}{\sqrt{|\zeta_1(0)|}} \\ t_0 = \sqrt{\frac{2|\zeta_1(0)|}{|b|u_{\max} - M}} \end{cases} \tag{52}$$

and is equal to:

$$t_f = \frac{3}{2}\sqrt{\frac{2|\zeta_1(0)|}{|b|u_{\max} - M}}. \tag{53}$$

Now, let us consider the second edge of the admissible set, i.e., the line given as

$$t_0 = \frac{\sqrt{2(|b|u_{\max} - M)}}{\iota}. \tag{54}$$

Substituting value (54) into the Equation (18), we obtain:

$$t_f = \frac{\sqrt{2(|b|u_{\max} - M)}}{2\iota} + \sqrt{\frac{2|\zeta_1(0)|}{|b|u_{\max} - M}}. \tag{55}$$

Calculating the derivative of the above function with respect to ι:

$$\frac{\partial t_f}{\partial \iota} = -\frac{\sqrt{2(|b|u_{\max} - M)}}{2\iota^2} \tag{56}$$

we obtain that it is always negative; thus, t_f is a decreasing function and its smallest value is obtained for the maximum admissible ι. Therefore, again, the minimum of the regulation time is given as (53) and the optimal sliding line parameters are obtained for ι and t_0 as in Equations (52).

2. $t_f \leq t_0$.
In this case, the state reaches the desired point along the non-stationary switching curve and the regulation time is given by Equation (23). Calculating the derivative of this function with respect to ι, we obtain:

$$\frac{\partial t_f}{\partial \iota} = -\frac{\sqrt[4]{|\zeta_1(0)|}}{\sqrt{\iota^3}}. \tag{57}$$

This value is always negative. Hence, again the minimum regulation time will be obtained for the maximum admissible value of ι. From inequality (34), we obtain that:

$$\iota = \frac{|b|u_{\max} - M}{2\sqrt{|\zeta_1(0)|}}. \tag{58}$$

Substituting the above value into Equation (23), we obtain the minimum regulation time:

$$t_f = 2\sqrt{\frac{2|\zeta_1(0)|}{|b|u_{\max} - M}}. \tag{59}$$

Comparing the minimum values of the regulation time, we conclude that the value (53) is always smaller than value (59). Hence, the optimal strategy is the one in which the switching curve stops during the control process. This ends the proof. □

3.4.2. Settling Time Minimization with the Velocity Constraint

In this subsection, our goal is to derive the minimal regulation time, for which the absolute value of the system's velocity is bounded from above by value $\zeta_{2\max}$ for any $t \geq 0$.

Theorem 3. *If the absolute value of the system's velocity is limited from above by $\zeta_{2\max}$ for any $t \geq 0$, then the minimum regulation time is:*

$$t_f = \frac{8\sqrt{3}|\zeta_1(0)|}{9\zeta_{2\max}} \tag{60}$$

and the optimal sliding line parameter value is:

$$\iota = \frac{27x_{2\max}^2}{16\sqrt{|\zeta_1(0)|^3}}. \tag{61}$$

The most beneficial strategy is the one in which the switching curve moves for the whole regulation process.

Proof. Using the proof of Theorem 2, we deduce that the minimum of the regulation time is obtained on the edge of the admissible set. Again, we consider two cases:

1. $t_f > t_0$.
Using inequality (40), we obtain the maximum value of ι equal to:

$$\iota = \frac{27x_{2\max}^2}{16\sqrt{|\zeta_1(0)|^3}}. \tag{62}$$

Substituting the above value into Equation (41), we obtain the optimal parameter t_0:

$$t_0 = \frac{8|\zeta_1(0)|}{9\zeta_{2\max}}. \tag{63}$$

Substituting values (62) and (63) into Equation (18), we conclude that, in this case, the minimum regulation time is

$$t_f = \frac{16|\zeta_1(0)|}{9\zeta_{2\max}}. \tag{64}$$

2. $t_f \leq t_0$.
In this case, the minimum value of the settling time is obtained for the maximum value of ι. Again, using inequality (40), we conclude that this value is given by (62). Substituting that value into Equation (23), we obtain the minimum value of the regulation time equal to t_0 given as (63).

Comparing both cases, we notice that (63) is always smaller than (64). Hence, the optimal strategy is the one in which the sliding line moves for the whole control process. This ends the proof. □

3.4.3. Settling Time Minimization with Both Control Signal and Velocity Constraints

In this subsection, the regulation time will be minimized in the case when the control signal and the system's velocity are both constrained.

Theorem 4. *If the absolute values of the control signal and the system's velocity are both bounded from above by $u_{\max}$ and $\zeta_{2\max}$, respectively, for any $t \geq 0$, then the minimum regulation time is equal to one of three values:*

$$t_f = \frac{3}{2}\sqrt{\frac{2|\zeta_1(0)|}{|b|u_{\max} - M}}, \tag{65}$$

$$t_f = \frac{8\sqrt{3}|\zeta_1(0)|}{9\zeta_{2\max}}, \tag{66}$$

$$t_f = \frac{8\sqrt{2(|b|u_{\max} - M)|\zeta_1(0)|^3}}{27x_{2\max}^2} + \sqrt{\frac{2|\zeta_1(0)|}{|b|u_{\max} - M}}. \tag{67}$$

and the optimal sliding line parameters are:

$$\begin{cases} \iota = \min\left\{\frac{|b|u_{\max}-M}{\sqrt{|\zeta_1(0)|}}; \frac{27x_{2\max}^2}{16\sqrt{|\zeta_1(0)|^3}}\right\} \\ t_0 = \max\left\{\sqrt{\frac{2|\zeta_1(0)|}{|b|u_{\max}-M}}; \min\left\{\frac{8\sqrt{3}|\zeta_1(0)|}{9\zeta_{2\max}}; \frac{16\sqrt{2(|b|u_{\max}-M)|\zeta_1(0)|^3}}{27x_{2\max}^2}\right\}\right\} \end{cases} \tag{68}$$

The most advantageous strategy is the one in which the switching curve stops during the regulation process.

Proof. Again, using the proof of Theorem 2, we conclude that the regulation time is a decreasing function of ι. Therefore, its minimum value is obtained on the edge of the admissible set. We will consider two cases:

1. $t_f > t_0$.
The first step will be to determine the intersection point of lines describing the maximum admissible t_0. Equating the right-hand sides of inequality (28) and Equation (41), we find that these lines cross for:

$$\iota = \frac{3(|b|u_{\max} - M)}{2\sqrt{|\zeta_1(0)|}}. \tag{69}$$

Using inequality (33), we can conclude that the above ι does not belong to the admissible set. Therefore, one of the t_0 functions in the admissible set is always greater than the other one. Let us observe that if ι increases, then the function:

$$t_0 = \frac{\sqrt{2(|b|u_{\max} - M)}}{\iota} \tag{70}$$

decays to zero faster than:

$$t_0 = \frac{2\sqrt{3}\sqrt[4]{|\zeta 1(0)|}}{3\sqrt{\iota}}. \tag{71}$$

Hence, in the admissible set, value (70) is always greater than value (71). Selecting the maximum admissible value of ι and then of t_0, we conclude that the limitation of the system's velocity will be fulfilled without any excess. In order to calculate the minimum value of the regulation time, we will analyze the edge of the admissible set described by the line:

$$\iota = \min\left\{\frac{|b|u_{\max} - M}{\sqrt{|\zeta_1(0)|}}; \frac{27x_{2\max}^2}{16\sqrt{|\zeta_1(0)|^3}}\right\}. \tag{72}$$

Substituting the above ι into Equation (18) and calculating its derivative with respect to t_0, one obtains:

$$\frac{\partial t_f}{\partial t_0} = \frac{1}{2} - \frac{2\sqrt{|\zeta_1(0)|}}{\min\left\{\frac{|b|u_{\max}-M}{\sqrt{|\zeta_1(0)|}}; \frac{27x_{2\max}^2}{16\sqrt{|\zeta_1(0)|^3}}\right\} t_0^2}. \tag{73}$$

Equating the right-hand side of formula (73) to 0, we obtain that the minimized regulation time is obtained for:

$$\begin{aligned} t_0 &= \frac{2\sqrt[4]{|\zeta_1(0)|}}{\sqrt{\min\left\{\frac{|b|u_{\max}-M}{\sqrt{|\zeta_1(0)|}}; \frac{27x_{2\max}^2}{16\sqrt{|\zeta_1(0)|^3}}\right\}}} \\ &= \max\left\{2\sqrt{\frac{|\zeta_1(0)|}{|b|u_{\max} - M}}; \frac{8\sqrt{3}|\zeta_1(0)|}{9\zeta_{2\max}}\right\}. \end{aligned} \tag{74}$$

Moreover, in order to constrain the control signal for the whole control process, we have to take into account that t_0 must satisfy condition (51). Let us observe that the right-hand side of the inequality (51) is smaller than the left-hand side in the maximum function of formula (74). Moreover, we have to consider the t_0 limitation given by inequality (28). Therefore, the minimum of the regulation time is obtained for:

$$\begin{cases} \iota = \min\left\{\frac{|b|u_{\max}-M}{\sqrt{|\zeta_1(0)|}}; \frac{27x_{2\max}^2}{16\sqrt{|\zeta_1(0)|^3}}\right\} \\ t_0 = \max\left\{\sqrt{\frac{2|\zeta_1(0)|}{|b|u_{\max}-M}}; \min\left\{\frac{8\sqrt{3}|\zeta_1(0)|}{9\zeta_{2\max}}; \frac{16\sqrt{2(|b|u_{\max}-M)|\zeta_1(0)|^3}}{27x_{2\max}^2}\right\}\right\} \end{cases} \tag{75}$$

Let us derive the minimum value of the regulation time. If:

$$\iota = \frac{|b|u_{\max} - M}{\sqrt{|\zeta_1(0)|}}, \tag{76}$$

then:

$$t_0 = \sqrt{\frac{2|\zeta_1(0)|}{|b|u_{\max} - M}}, \tag{77}$$

however, if:

$$\iota = \frac{27x_{2\max}^2}{16\sqrt{|\zeta_1(0)|^3}}, \tag{78}$$

then:

$$t_0 = \frac{8\sqrt{3}|\zeta_1(0)|}{9\zeta_{2\max}} \tag{79}$$

or:

$$t_0 = \frac{16\sqrt{2(|b|u_{\max} - M)|\zeta_1(0)|^3}}{27x_{2\max}^2}. \tag{80}$$

We will substitute proper values of ι and t_0 into Equation (18):

- $\iota = \frac{|b|u_{\max} - M}{\sqrt{|\zeta_1(0)|}}$ and $t_0 = \sqrt{\frac{2|\zeta_1(0)|}{|b|u_{\max} - M}}$. In this case:

$$t_f = \frac{3}{2}\sqrt{\frac{2|\zeta_1(0)|}{|b|u_{\max} - M}}. \tag{81}$$

- $\iota = \frac{27x_{2\max}^2}{16\sqrt{|\zeta_1(0)|^3}}$ and $t_0 = \frac{8\sqrt{3}|\zeta_1(0)|}{9\zeta_{2\max}}$. Then:

$$t_f = \frac{8\sqrt{3}|\zeta_1(0)|}{9\zeta_{2\max}}. \tag{82}$$

- $\iota = \frac{27x_{2\max}^2}{16\sqrt{|\zeta_1(0)|^3}}$ and $t_0 = \frac{16\sqrt{2(|b|u_{\max} - M)|\zeta_1(0)|^3}}{27x_{2\max}^2}$. In this case:

$$t_f = \frac{8\sqrt{2(|b|u_{\max} - M)|\zeta_1(0)|^3}}{27x_{2\max}^2} + \sqrt{\frac{2|\zeta_1(0)|}{|b|u_{\max} - M}}. \tag{83}$$

We were not able to decide which of three values (81)–(83) is the smallest one, since they depend on $u_{\max}$, $\zeta_{2\max}$, $|\zeta_1(0)|$ and b. However, these parameters are well-known from the beginning of the regulation process. Hence, after substituting these values, we can derive the minimum value of the regulation time.

2. $t_f \leq t_0$.

In this case, the minimum of the regulation time will again be obtained for the maximum value of parameter ι. In order to constrain both the input and system's velocity, both inequalities (34) and (40) must hold. We have to select the more restrictive constraint. Hence:

$$\iota = \min\left\{\frac{|b|u_{\max} - M}{2\sqrt{|\zeta_1(0)|}}; \frac{27x_{2\max}^2}{16\sqrt{|\zeta_1(0)|^3}}\right\}. \tag{84}$$

Substituting the above value into Equation (23), we obtain the minimum value of the regulation time:

$$t_f = \max\left\{2\sqrt{\frac{2|\zeta_1(0)|}{|b|u_{\max} - M}}; \frac{8\sqrt{3}|\zeta_1(0)|}{9\zeta_{2\max}}\right\}. \tag{85}$$

In order to determine which strategy is the most beneficial, we have to compare values (81)–(83) to the value (85). It is easy to see that (81) is always smaller than the first value in the maximum function in (85). Moreover, (82) is equal to the second value in that maximum function. The regulation time given by formula (83) satisfies the inequalities:

$$\begin{aligned} t_f &\leq \frac{1}{2}\left(\frac{8\sqrt{3}|\zeta_1(0)|}{9\zeta_{2\max}} + 2\sqrt{\frac{2|\zeta_1(0)|}{|b|u_{\max} - M}}\right) \\ &\leq \max\left\{2\sqrt{\frac{2|\zeta_1(0)|}{|b|u_{\max} - M}}; \frac{8\sqrt{3}|\zeta_1(0)|}{9\zeta_{2\max}}\right\}. \end{aligned} \tag{86}$$

Hence, the regulation time given by Equation (83) is always smaller than the value (85). To sum up—each of values (81)–(83) is smaller than or equal to (85). Therefore, the most advantageous option is the one in which the sliding line stops during the regulation process. This ends the proof. □

4. Simulation Example

In this section, a simulation example of controlling a single link of a robotic manipulator will be demonstrated. For the control of the full manipulator, one would have to apply a similar controller for every joint of that manipulator. We consider a single rotary link, working in a vertical plane, which is described by

$$\begin{cases} \frac{d}{dt}\zeta_1(t) = \zeta_2(t) \\ \frac{d}{dt}\zeta_2(t) = \frac{1}{J}\{mgr\sin[\zeta_1(t)] + d(t) + u(t)\} \end{cases}, \tag{87}$$

where ζ_1 is an angular position expressed in radians and ζ_2 is an angular velocity expressed in radians per second. The moment of inertia $J = 1$ kg $\cdot$ m^2, the single link mass $m = 4$ kg and the distance from the mass center to the pivot point is $r = 0.4$ m. Figure 1 presents the scheme of the system.

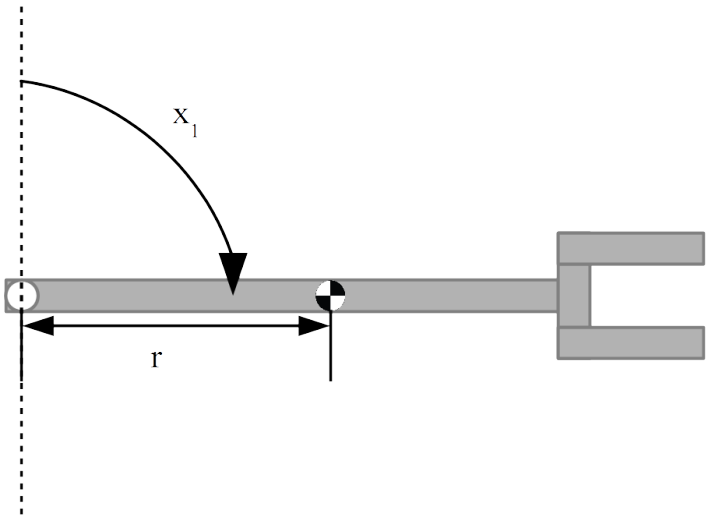

Figure 1. Scheme of the system.

Function d is an unknown disturbance with a bounded amplitude with the opposite sign to the velocity. In this way, the torque of resistance in bearings was modeled. It takes a value from $[0;1]$ Nm. From the fact that $mgr = 16$ Nm and the range of disturbances, we obtain that $M = 17$ Nm. The limitation of the control signal is $u_{\max} = 70$ Nm, and the limitation of the system's velocity is $\zeta_{2\max} = 8\ \frac{\text{rad}}{\text{s}}$. The starting position of the robot's manipulator is equal to π and our goal is to rotate it to the zero position. In simulations, we considered a continuous-time model, namely the computation step, which was selected as small enough to represent the behavior of a continuous-time system. In order to be applicable in practice, the controller would obviously have to be discretized using some well-known methods. We did not present this discretization here, to maintain the brevity and clarity of the paper.

4.1. Control Signal Constraint

In this case, the optimal parameters of the sliding line are:

$$\begin{cases} \iota \approx 29.9096 \\ t_0 \approx 0.3442 \end{cases} \tag{88}$$

and the optimal settling time is:

$$t_f \approx 0.5163. \tag{89}$$

The presented parameter values (88) are the result of the optimization process. However, the controller ensures the robustness and stability for any positive ι and t_0. If, for some reason (e.g., limited computational precision), the exact values were not used, the only drawback would be a sub-optimal settling time.

Figure 2 presents the control signal. We can see that its maximum admissible range was utilized. Its average value rises monotonically to the moment t_0. After the sliding line stops, the control signal switches between 36 Nm and 70 Nm. When the state reaches the desired point, the control signal takes a value of -17 Nm or 17 Nm. All oscillations arise as a result of maintaining the state on the switching curve for the whole control process, and in the demand state after t_f. The amplitude of this oscillation is equal to $\frac{M}{b} = 17$ Nm. Evidently, in practice, the chattering would have to be reduced, using one of the known methods. We have not done so in order to present the main results in a clear, concise way.

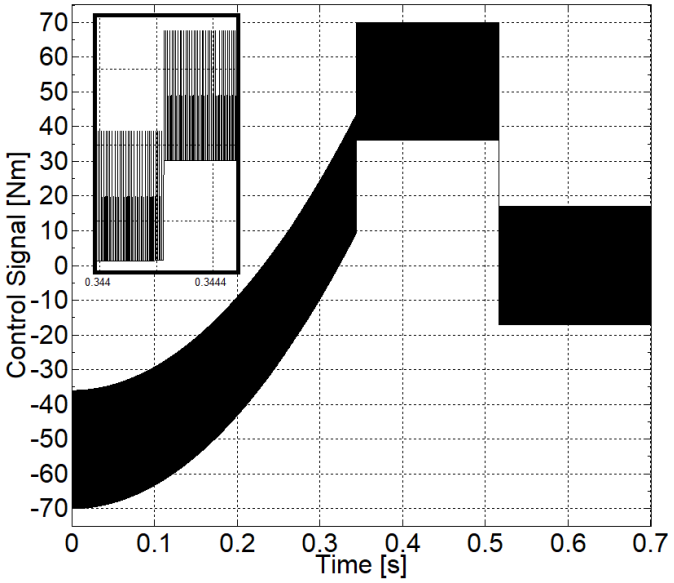

Figure 2. Control signal with the input constraint.

From Figure 3, one can notice that the system's angular position decreases monotonically from its initial value to the demand value and reaches it at the time t_f.

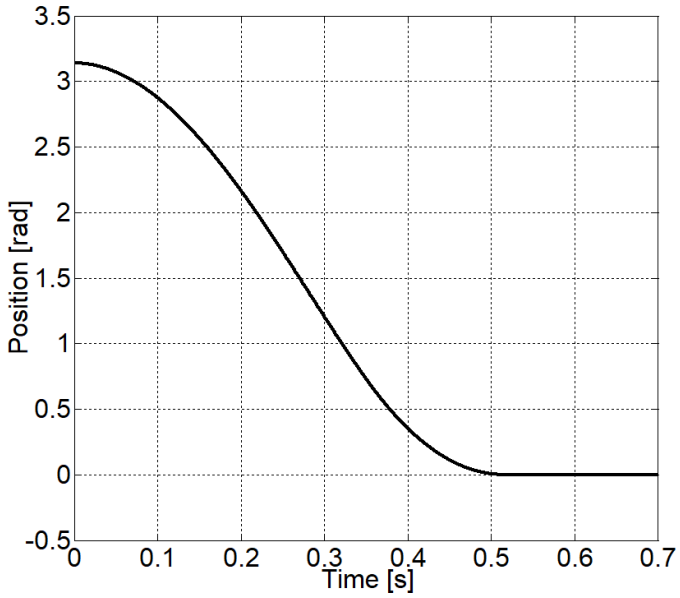

Figure 3. System's position with the input constraint.

System's angular velocity is presented in Figure 4. Starting from its initial value, it decreases to its minimum value, then it becomes an increasing function until it achieves its demand value $0\frac{\text{rad}}{\text{s}}$ in finite time.

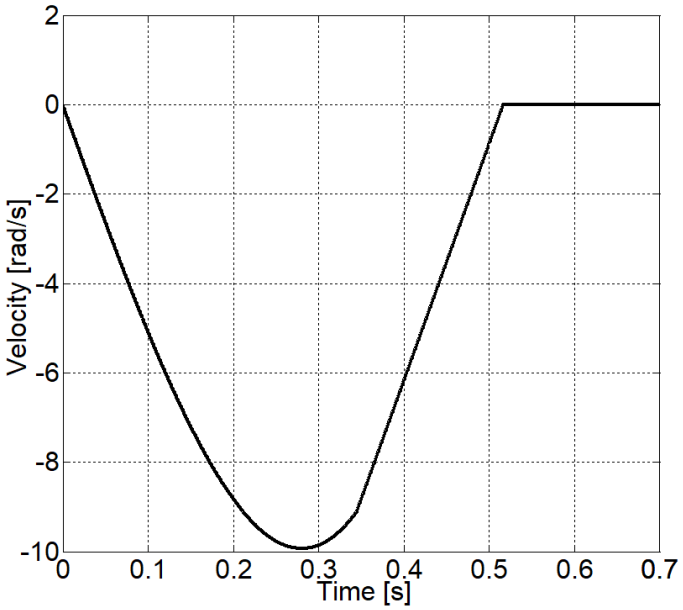

Figure 4. System's velocity with the input constraint.

From Figure 5, one can observe that the system is insensitive to the external disturbances for the entire control process.

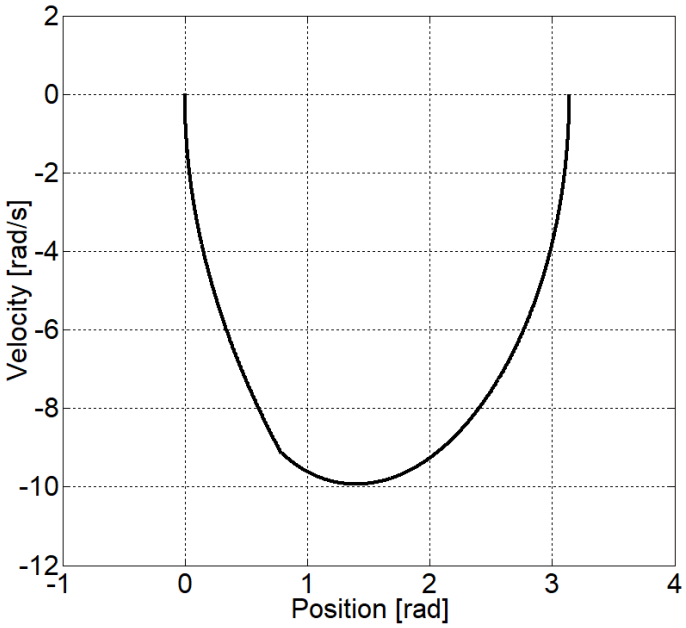

Figure 5. State trajectory with the input constraint.

4.2. System's Angular Velocity Constraint

When the angular velocity is limited for the whole regulation process, then:

$$\iota \approx 19.4102 \tag{90}$$

and the optimal settling time is:

$$t_f \approx 0.6043. \tag{91}$$

Figure 6 presents the control signal in the case when the system's angular velocity is constrained. One can observe that its minimum and maximum values are both higher than those shown in Figure 2. The best strategy is the one in which the sliding line is non-stationary for the entire control process. Therefore, the average value of the control signal rises monotonically until the state reaches the desired point. After that, it switches between −17 Nm and 17 Nm.

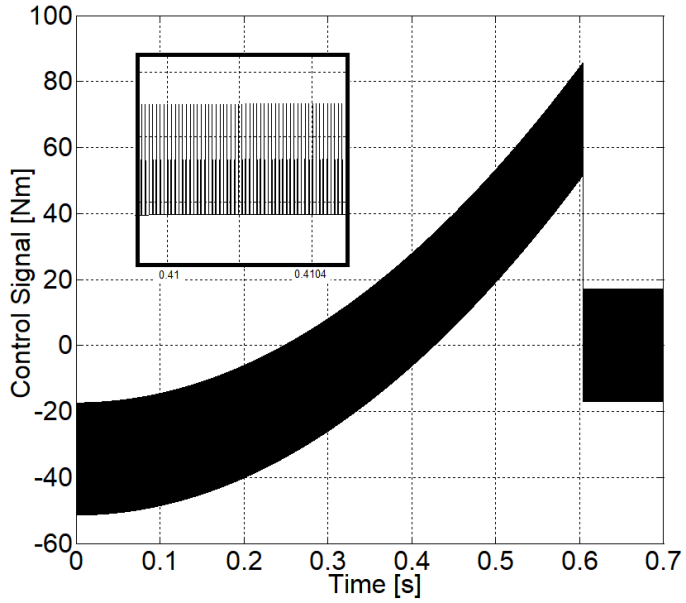

Figure 6. Control signal with the velocity constraint.

The system's angular position graph shown in Figure 7 is similar to the one presented in Figure 3. However, the demand state is reached subsequently.

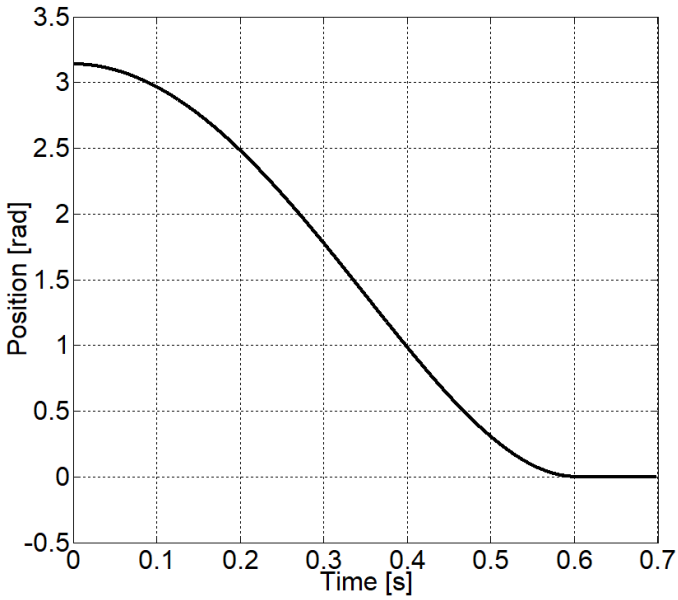

Figure 7. System's position with the velocity constraint.

In this case, the system's angular velocity shown in Figure 8 reaches its minimum admissible value; after that, it recovers and attains the desired state at t_f.

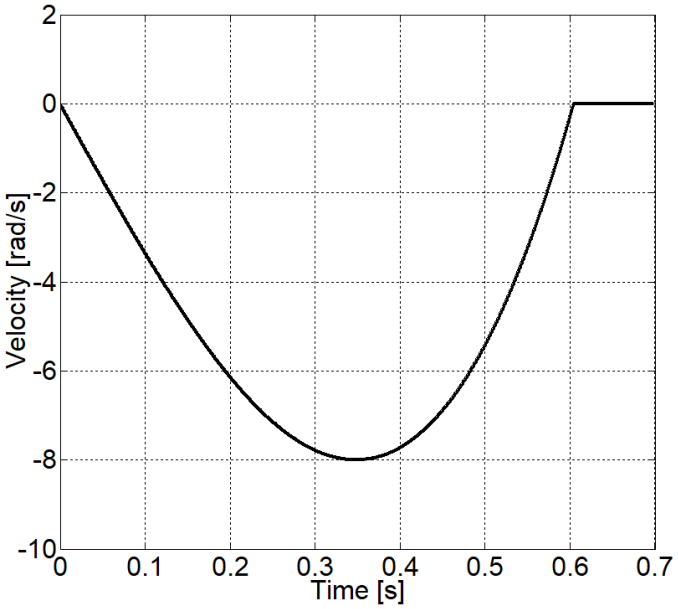

Figure 8. System's velocity with the velocity constraint.

Again, from Figure 9 we conclude that the system is insensitive to perturbations for the entire control process.

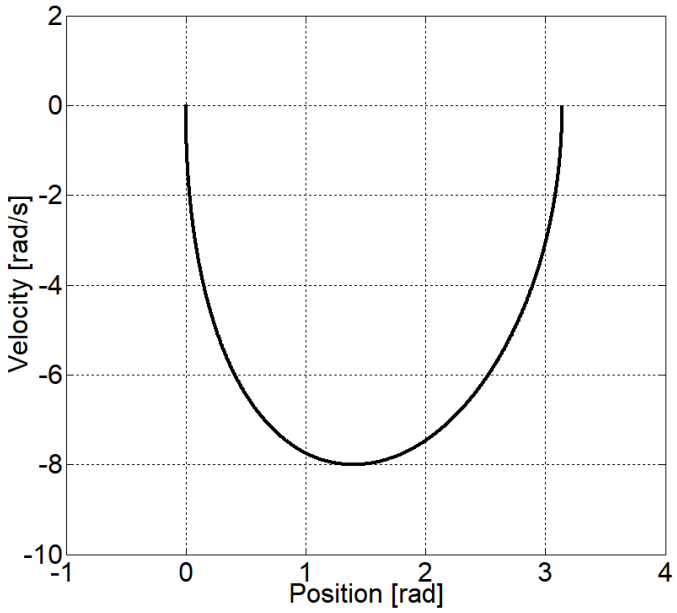

Figure 9. State trajectory with the velocity constraint.

4.3. Both Control Signal and System's Angular Velocity Constraints

In this case, the optimal parameters of the sliding line are given by

$$\begin{cases} \iota \approx 19.4102 \\ t_0 \approx 0.5304 \end{cases} \tag{92}$$

and the optimal settling time is:

$$t_f \approx 0.6094. \tag{93}$$

One can observe that, in this case, the settling time has the greatest value, which is a reasonable result, because now we have to satisfy not one, but two constraints.

Now, the initial value of the control signal visible in Figure 10 is equal to the one in the case when only the system's angular velocity is constrained. After that, its average value increases to the moment t_0 and after that it switches again between 36 Nm and 70 Nm in order to maintain the control signal constraint.

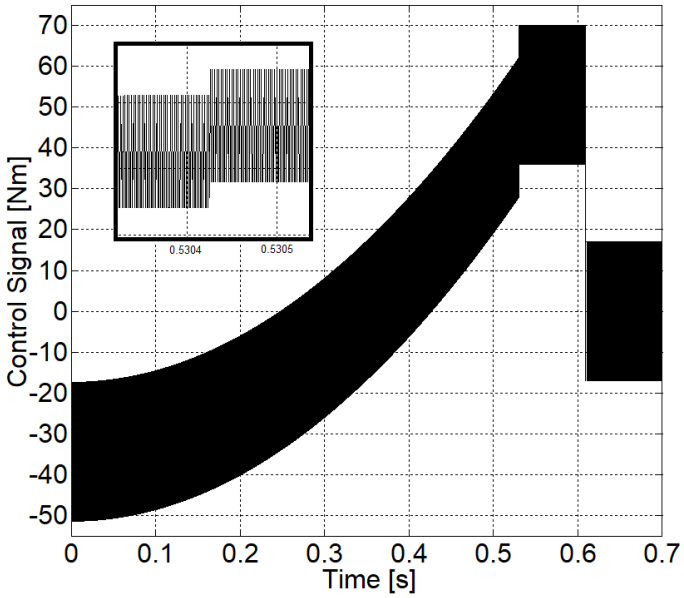

Figure 10. Control signal with both input and velocity constraints.

System's angular position graph is given in Figure 11. Again, its shape is similar to the ones presented in Figures 3 and 7.

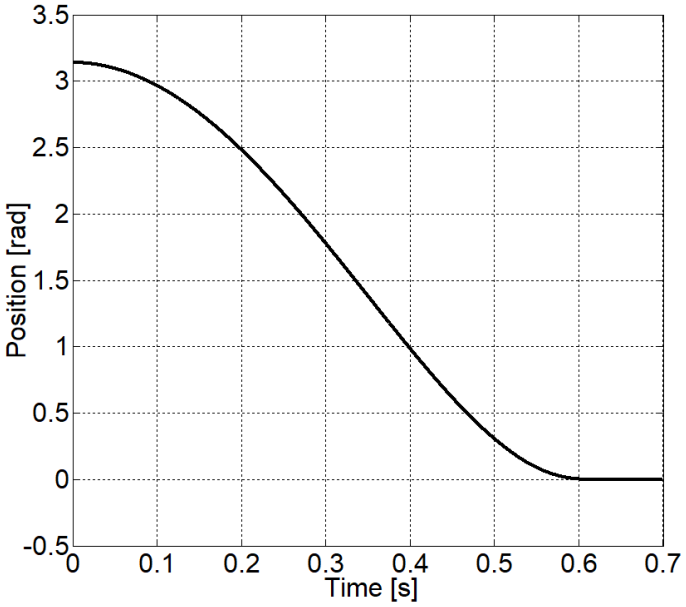

Figure 11. System's position with both input and velocity constraints.

The system's angular velocity shown in Figure 12 satisfies its constraint, and after reaching its minimum value, it increases until the state reaches the desired point.

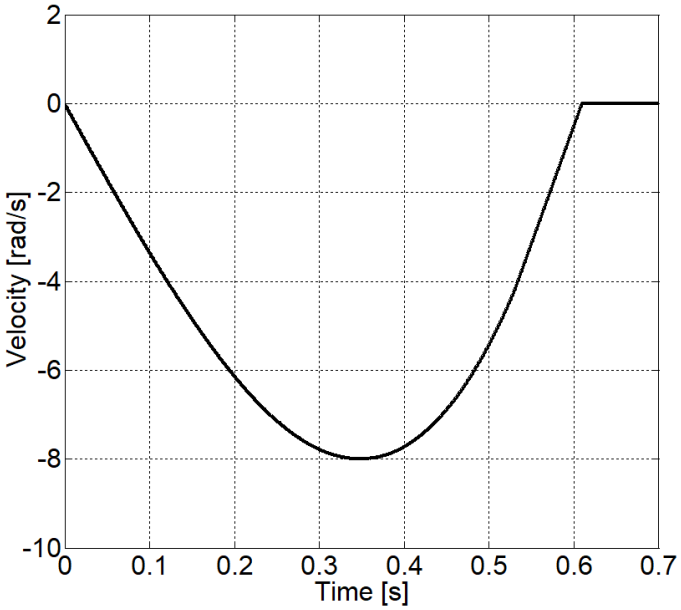

Figure 12. System's velocity with both input and velocity constraints.

Again, in Figure 13 one can see that in all three cases, our system is insensitive to perturbations. Table 1 presents the comparison of some well-known quality indices: settling time, IAE and ITAE computed for three simulation scenarios.

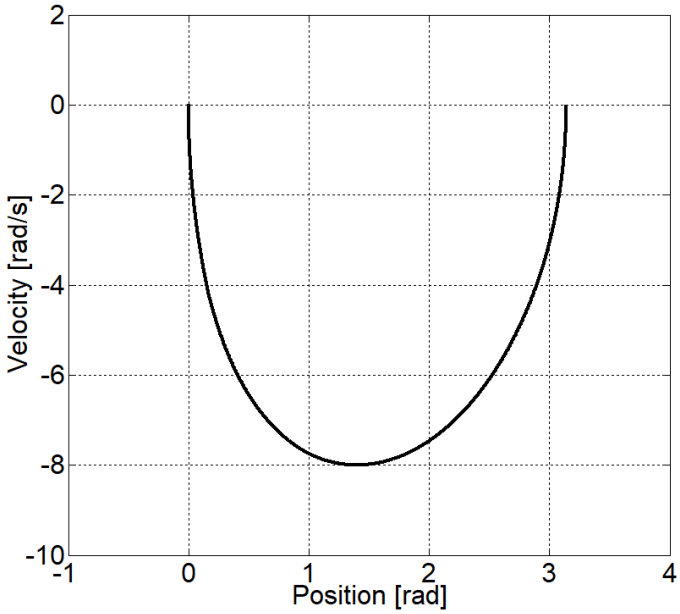

Figure 13. State trajectory with both input and velocity constraints.

Table 1. Comparison of well-known quality indices.

	t_f	IAE	ITAE
u limitation	0.5163	0.8197	0.1260
ζ_2 limitation	0.6043	1.0120	0.1911
both limitations	0.6094	1.0121	0.1912

5. Conclusions

In this paper, we proposed a terminal continuous-time sliding mode controller. It was stated and proven that the presented control signal ensures the stable sliding motion for the entire control process. In order to remove the reaching phase, the time-variant switching curve was introduced. The controller guarantees the finite-time convergence of the state to the desired point. In our work, three types of constraints were considered: a control signal constraint, a system velocity constraint and both of these constraints combined. In order to assess the dynamical behavior of the system, a settling time was selected as a quality index. It was minimized in the three mentioned cases. In the end, the simulation example that included the control of a single joint of a robotic manipulator was presented. These simulations verified the theoretical considerations shown in this paper. In future work, we will include noisy measurements, non-zero initial speed as well as comparing our approach with some similar controllers.

Author Contributions: Conceptualization, A.B., and M.P.; methodology, M.P. and A.B.; validation, M.P. and P.L.; formal analysis, M.P. and P.L.; investigation, M.P. and P.L.; writing—original draft preparation, M.P. and P.L; writing—review and editing, A.B.; visualization, M.P.; supervision, A.B. and P.L. All authors have read and agreed to the published version of the manuscript.

Funding: This research received no external funding.

Data Availability Statement: Data sharing not applicable.

Conflicts of Interest: The authors declare no conflict of interest.

References

1. Basin, M.; Fridman, L.; Shi, P. (Eds.) Optimal sliding mode algorithms for dynamic systems. *J. Frankl. Inst.* **2012**, *349*, 1317–1616. [CrossRef]
2. Gao, W. (Ed.) Variable structure control. *IEEE Trans. Ind. Electron.* **1993**, *40*, 1–165.

3. Kaynak, O.; Bartoszewicz, A.; Utkin, V.I. (Eds.) Sliding mode control in industrial applications. *IEEE Trans. Ind. Electron.* **2009**, *56*, 3271–3274.
4. Misawa, A.; Utkin, V.I. (Eds.) Variable structure systems. *Trans. Asme J. Dyn. Syst. Meas. Control.* **2000**, *122*, 585–819.
5. Utkin, V.I. (Ed.) Sliding mode control. *Int. J. Control* **1993**, *57*, 1003–1259.
6. Shtessel, Y.; Spurgeon, S.; Fridman, L. Advances in sliding mode observation and estimation. *Intern. J. Syst. Sci.* **2007**, *38*, 845–942. [CrossRef]
7. Utkin, V.I. Variable structure systems with sliding modes. *IEEE Trans. Autom. Control* **1977**, *22*, 212–222. [CrossRef]
8. Furuta, K. Sliding mode control of a discrete system. *Syst. Control Lett.* **1990**, *14*, 145–152. [CrossRef]
9. Milosavljević, Č. General conditions for the existence of a quasisliding mode on the switching hyperplane in discrete variable structure systems. *Autom. Remote. Control* **1985**, *46*, 307–314.
10. Utkin, V.I.; Drakunow, S.V. On discrete-time sliding mode control. *IFAC Conf. Nonlinear Control* **1989**, 484–489.
11. Choi, S.B.; Park, D.W.; Jayasuriya, S. A time-varying sliding surface for fast and robust tracking control of second-order uncertain systems. *Automatica* **1994**, *30*, 899–904. [CrossRef]
12. Yilmaz, C.; Hurmuzlu, Y. Eliminating the reaching phase from variable structure control. *J. Dyn. Syst. Meas. Control.* **2000**, *122*, 753–757. [CrossRef]
13. Man, Z.; Yu, X.H. Terminal sliding mode control of MIMO linear systems. *IEEE Trans. Circuits Syst. I Fundam. Theory Appl.* **1997**, *44*, 1065–1070.
14. Man, Z.; Paplinski, A.; Wu, H.R. A robust MIMO terminal sliding mode control scheme for rigid robotic manipulators. *IEEE Trans. Autom. Control* **1994**, *39*, 2464–2469.
15. Tang, Y. Terminal sliding mode control for rigid robots. *Automatica* **1998**, *34*, 51–56. [CrossRef]
16. Hosseinzadeh, M.; Cotorruelo, A.; Limon, D.; Garone E. Constrained Control of Linear Systems Subject to Combinations of Intersections and Unions of Concave Constraints. *IEEE Control Syst. Lett.* **2019**, *3*, 571–576. [CrossRef]
17. O'Rourke, I.; Kolmanowvsky, I.; Garone, E.; Girard, A. Explicit Reference Governor for Constrained Maneuver and Shape Control of a Seven-State Multibody Aircraft. In *AIAA Scitech 2020 Forum*; AIAA: Reston, VA, USA, 2020; p. 1830.
18. Gao, P.; Zhang, G.; Lv, X. Model-Free Control Using Improved Smoothing Extended State Observer and Super-Twisting Nonlinear Sliding Mode Control for PMSM Drives. *Energies* **2021**, *14*, 922. [CrossRef]
19. Milosavljević, Č.; Peruničić-Draženović B.; Veselić, B.; Petronijević, M. High-performance discrete-time chattering-free sliding mode-based speed control of induction motor. *Electr. Eng.* **2017**, *99*, 583–593. [CrossRef]
20. Kali, Y.; Saad, M.; Doval-Gandoy, J.; Rodas, J. Discrete terminal super-twisting current control of a six-phase induction motor. *Energies* **2021**, *14*, 1339. [CrossRef]
21. Ali, N.; Liu, Z.; Armghan, H.; Ahmad, I.; Hou, Y. LCC-S-Based integral terminal sliding mode controller for a hybrid energy storage system using a wireless power system. *Energies* **2021**, *14*, 1693. [CrossRef]
22. Mobayen, S.; Bayat, F.; Lai, C.-C.; Taheri, A.; Fekih, A. Adaptive global sliding mode controller design for perturbed DC-DC buck converters. *Energies* **2021**, *14*, 1249. [CrossRef]
23. Oliveira, T.; Caseiro, L.; Mendes, A.; Cruz, S.; Perdigão, M. Model Predictive Control for Paralleled Uninterruptible Power Supplies with an Additional Inverter Leg for Load-Side Neutral Connection. *Energies* **2021**, *14*, 2270. [CrossRef]
24. Vásquez, L.O.P.; Ramírez, V.M.; Langarica Córdova, D.; Redondo, J.L.; Álvarez, J.D.; Torres-Moreno, J.L. Optimal Management of a Microgrid with Radiation and Wind-Speed Forecasting: A Case Study Applied to a Bioclimatic Building. *Energies* **2021**, *14*, 2398. [CrossRef]